PAX6 dosage effects on comeal development, growth, and wound healing

Published in final edited form as:
Dev Dyn. 2008 May ; 237(5): 1295–1306. doi:10.1002/dvdy.21528.

PAX6 Dosage Effects on Corneal Development, Growth, and Wound Healing

Natalie Dorà[1], **Jingxing Ou**[1], **Romana Kucerova**[1], **Ida Parisi**[1], **John D. West**[2], and **J. Martin Collinson**[1,*]

[1]School of Medical Sciences, University of Aberdeen, Institute of Medical Sciences, Foresterhill, Aberdeen, United Kingdom

[2]Division of Reproductive and Developmental Sciences, The University of Edinburgh Genes and Development Group, Hugh Robson Building, George Square, Edinburgh, United Kingdom

Abstract

The requirement for correct dosage of the transcription factor Pax6 during corneal growth and development was investigated using the Pax6-overexpressing (*PAX77*) transgenic mouse. Transgenics had a microcornea phenotype due to failure of postnatal growth, associated with reduction in the number of cells layers in the corneal epithelium. Cell cycle progression was monitored using bromodeoxyuridine, p63, cyclin E, and phosphohistone-3 labeling: proliferation rates were higher in *PAX77*$^{+}$ than wild-type, without a concomitant increase in apoptosis. Hence, failure of proliferation did not underlie microcornea. *PAX77*$^{+}$ corneal epithelia had reduced levels of cytokeratin-12, and exhibited severe wound healing delay that, in contrast to *Pax6*$^{+/-}$ mice, could not be modulated by exogenous growth factors. *PAX77*$^{+}$ lenses showed partial failure of lens fiber differentiation. The data demonstrate that anterior eye development is very sensitive to Pax6 dosage. Although there are similarities between the eye phenotype of *Pax6* heterozygotes and overexpressing mice, there are also striking differences.

Keywords

cornea; Pax6; gene dosage; anterior segment; wound healing

INTRODUCTION

Development of the mammalian cornea, in terms of growth, stratification, differentiation, and initiation of patterns of cell migration is substantially a postnatal event, taking several months even in mice (Collinson et al., 2002). The *PAX6* gene encodes a transcription factor, essential for normal development of the mammalian eye (e.g., Ton et al., 1991; Hill et al., 1991; Grindley et al., 1995). *Pax6* expression is down-regulated in many adult tissues, but it is maintained in the corneal epithelium (Koroma et al., 1997), where it is involved in maintenance and in wound healing (Chao et al., 2000; Sivak et al., 2000; Sivak et al., 2004; Baulmann et al., 2002; Davis et al., 2003; Leiper et al., 2006; Ramaesh et al., 2006). Corneal abnormalities of the Pax6 heterozygous mouse have been well documented (Baulmann et al., 2002; Davis et al., 2003; Ramaesh et al., 2003, 2005a, 2006) and are similar to the changes seen in human *PAX6*$^{+/-}$ aniridia (Nishida et al., 1995). Aniridia is a sight-

*Correspondence to: J. Martin Collinson, School of Medical Sciences, University of Aberdeen, Institute of Medical Sciences, Foresterhill, Aberdeen AB25 2ZD, UK. E-mail: m.collinson@abdn.ac.uk.

Europe PMC Funders Author Manuscripts

threatening bilateral pan-ocular condition in which the development of the iris, retina, lens, and cornea is disturbed (Shaw, 1960; Nelson et al., 1984; Churchill et al., 2000; Ramaesh at al., 2005b). Marked changes in the corneal epithelium are seen in aniridic patients, which can culminate in corneal opacification leading to visual loss (Nelson et al., 1984, Ramaesh et al., 2005b).

Limbal stem cell deficiency is in part responsible for the corneal changes in *PAX6*$^{+/-}$ individuals (Cotsarelis et al., 1996; Holland et al., 2003; Collinson et al., 2004; Ramaesh et al., 2005b). However, other factors play a role, including abnormal corneal differentiation leading to fragility of corneal epithelial cells, an abnormal epithelial response to wounding due to inefficient cell-cell signalling mechanisms, and abnormal cell migration and adhesion (Davis et al., 2003; Collinson et al., 2004; Ramaesh et al., 2005a; Leiper at al., 2006; Kucerova et al., 2006).

The production of the *PAX77* transgenic mouse model (Schedl et al., 1996) suggested that *Pax6* overexpression also interfered with normal eye development. Schedl et al. (1996) showed that there is a reduction in overall eye size in *PAX77*$^{+}$ mice, which carry five to seven copies of a 500-Mb YAC-based transgene containing the human *PAX6* locus and overexpressing *PAX6* in a tissue-specific pattern that recapitulates that of the endogenous gene. The transgenic mice exhibited microcornea, and their corneas were transparent. Some of the features of the *PAX77* mouse described in Schedl et al. (1996; cataract, microphthalmia) suggested similarities to the *Pax6*$^{+/-}$ mouse. Thus, it was postulated that both under and overexpression of Pax6 lead to similar developmental defects.

Alternative splicing of exon 5a yields two major protein isoforms, Pax6 and Pax6(5a). Transgenic mice overexpressing human Pax6 or Pax6(5a) in the lens develop cataracts with abnormalities in fiber cell and shape as well as fiber cell/lens capsule and fiber cell/fiber cell interactions (Duncan et al., 2000, 2004). Relatively small changes in the Pax6 and Pax6(5a) ratio may be important, because the two isoforms affect different downstream target genes (Epstein et al., 1994). The overexpression of Pax6 or Pax6(5a) isoforms in various systems has highlighted the effects of specific isoforms on gene expression and eye development (Chauhan et al., 2002a,b; Pinson et al., 2005). Therefore, the regulation of the relative levels of the two isoforms is very important for normal development (Duncan et al., 2004). The intact Pax6 locus is subject to positive autoregulation and this might provide a mechanism that stabilizes the relative levels of the two major isoforms of Pax6 (Duncan et al., 2004).

Aalfs et al. (1997) reported a human case of *PAX6* overexpression due to duplication of chromosome band 11p12→13, which includes the Wilms' tumor gene (WT1) and *PAX6*. This resulted in borderline developmental abnormalities, mild facial anomalies, and eye abnormalities. A reduction in overall eye size was reported along with transparent, small corneas. The phenotypic features of the *PAX77* mouse (Schedl et al., 1996) are comparable to those seen in the duplication of human 11p12→13, suggesting a detrimental effect of extra copies of *PAX6* on eye development in both mice and humans (Aalfs et al., 1997). The *PAX77* mouse is, therefore, a model of human microcornea.

While it is clear that the overexpression of *Pax6* has an adverse effect on eye development, little work has focused on the effects of increased expression of *Pax6* on corneal structure and function. Therefore, the purpose of this study was to investigate the effects of *Pax6* overexpression for corneal development and function in the *PAX77* transgenic mouse model.

RESULTS

Histological Analysis of the Anterior Segment of the *PAX77*$^{+}$ Eyes

Hematoxylin and eosin staining of *PAX77*$^{+}$ eyes revealed morphological differences in the anterior segment compared with wild-type, although the corneas looked relatively normal in tissue section. At postnatal day (P) 2 in both genotypes, the corneal epithelium consisted of a single layer of cells. Stratification was evident at P10 (Fig. 1A,B), and two to six cell layers were observed in adults (Fig. 1C,D) (analyzed quantitatively below). Periodic acid-Schiff (PAS) reagent staining did not detect the presence of ectopic conjunctival goblet cells in the *PAX77*$^{+}$ corneal epithelia in contrast to *Pax6*$^{+/-}$ (Ramaesh et al., 2005a). Corneal stromal lamination and the collagen fiber lattice were normal in *PAX77*$^{+}$ (Fig. 1E,F). All *PAX77*$^{+}$ eyes at all ages lacked ciliary bodies (Fig. 1G,H). Irides of the *PAX77*$^{+}$ mice were hypertrophic in comparison to the wild-type, with cyst like structures as described by Schedl et al. (1996; Supplementary Figure S1, which can be viewed at http://www.interscience.wiley.com/jpages/10588388/suppmat).

Failure of Postnatal Growth and Fewer Cell Layers in the *PAX77*$^{+}$ Corneal Epithelium

At P2, corneal diameter was slightly, but significantly smaller in the *PAX77*$^{+}$ (mean ± SEM: 1.27 ± 0.024 mm; n = 10) than wild-type (1.49 ± 0.017 mm; n = 10; unpaired *t*-test: $P < 0.0001$). At older stages, the differences between wild-type and *PAX77*$^{+}$ were very obvious (Fig. 2A). Corneal diameter of P10 *PAX77*$^{+}$ mice was significantly smaller (mean ± SEM: 1.23 ± 0.0295 mm; n = 12) than wild-type (2.21 ± 0.061 mm; n = 12; unpaired *t*-test: $P < 0.0001$), and the size difference was particularly noticeable in adults (*PAX77*$^{+}$: 1.4 ± 0.06 mm, n = 12; wild-type: 3.39 ± 0.04 mm, n = 16; unpaired *t*-test: $P < 0.0001$). The etiology of *PAX77*$^{+}$ microcornea is, hence, a failure of postnatal growth following relatively normal embryonic development.

For quantitative analysis, transverse tissue sections of the corneal epithelium were divided into four equal regions as described in the Experimental Procedures section, with the two outer sectors representing the peripheral cornea and the two inner sectors the central cornea. In the adult *PAX77*$^{+}$ mice, the corneal epithelium was made up of fewer cell layers than wild-type in both central and peripheral areas of the cornea (*PAX77*$^{+}$ peripheral mean ± SEM: 2.77 ± 0.19 layers vs. wild-type 4.04 ± 0.12, $P < 0.001$ by unpaired *t*-test; *PAX77*$^{+}$ central mean ± SEM: 3.4 ± 0.27 vs. wild-type 4.8 ± 0.1, $P < 0.01$ by unpaired *t*-test). In some cases, the cell layers appeared to be disorganized when compared with the wild-type.

Morphometric analysis of adult tissue sections was performed (Fig. 2B). In both genotypes, the corneal epithelium was significantly thicker in central regions than at the periphery (paired *t*-test: $P < 0.001$ in the wild-type and $P < 0.05$ in *PAX77*$^{+}$). The *PAX77*$^{+}$ corneal epithelium was significantly thinner in peripheral regions compared with the wild-type (unpaired *t*-test: $P < 0.05$). Although fewer cell layers were detected in *PAX77*$^{+}$ corneal epithelial, there was no significant difference in thickness of the epithelium between the two genotypes in central corneal regions, suggesting a change in cell shape in the *PAX77*$^{+}$compared with wild-type. There were no differences seen in the thickness of the stroma and endothelium between the two genotypes.

Pax6 Expression in the *PAX77*$^{+}$ Eye Is Up-regulated

Pax6 was expressed in a tissue-appropriate manner in *PAX77*$^{+}$ eyes at all ages at levels higher than those observed for wild-type (Fig. 3). Western blot of adult corneas was performed and quantified against β-actin loading control, confirming that Pax6 was expressed at significantly higher levels in the *PAX77*$^{+}$ corneas at this age compared with wild-type littermates (mean 2.24-fold difference; Fig. 3B,C). The ratio of Pax6 : Pax6(5a)

isoforms was also quantified on Western blots, where, for wild-type adult controls. this ratio was 5.35 ±0.67 (n = 5) and for littermates was 3.97 ±0.45 (n = 7). The difference was not significant by Mann-Whitney *U* test ($U = 26$; $P = 0.20$). Semiquantitative immunohistochemical analysis for Pax6 expression (Leiper et al., 2006) was performed by measuring the intensity of fluorescence of individual nuclei from corneal sections of wild-type and *PAX77*$^+$ littermates after immunohistochemistry performed and photographed in parallel using an Alexa 488-tagged anti-mouse IgG1 secondary antibody. At postnatal day 2, before onset of phenotypic changes, mean nuclear fluorescence (derived from luminosity histogram, Adobe Photoshop, arbitrary units) of wild-type corneal epithelia was 34.6 ± 2.48 (n = 68), significantly less than that of *PAX77*$^+$, 56.3 ± 2.49 (*t*-test: $P < 0.0001$). By this estimate, *PAX77*$^+$ P2 neonates, therefore, expressed 1.63-fold more Pax6 in the corneal epithelium than their wild-type littermates.

Cell Cycle Progression Is Not Retarded in the *PAX77*$^+$ Corneal Epithelium

Because *PAX77*$^+$ corneas did not grow significantly after birth, cell proliferation was investigated in both eyes from four adult *PAX77*$^+$ mice and four adult wild-type mice by immunohistochemistry following intraperitoneal injection of bromodeoxyuridine (BrdU) as described in the Experimental Procedures section. In the corneal epithelium of both genotypes, BrdU-positive cells were restricted to the basal layer. In both wild-type and *PAX77*$^+$, the percentage of BrdU-positive cells in the corneal epithelium did not differ significantly from peripheral to central regions (paired *t* tests: wild-type $P = 0.35$, *PAX77*$^+$ $P = 0.87$). The percentage of S-phase cells (BrdU-positive nuclei) was significantly higher in the *PAX77*$^+$ epithelia in both the peripheral and central regions of the cornea (peripheral mean ± SEM: *PAX77*$^+$ = 13.42 ± 1.28%, wild-type = 7.66 ± 0.76%, $P < 0.001$ by unpaired *t*-test; central mean ± SEM: *PAX77*$^+$ = 13.85 ± 1.31%, wild-type = 6.11 ± 1.31, $P < 0.01$ by unpaired *t*-test; Fig. 4A,B).

Antisera against phospho-histone H3 (PH3) were used to detect mitotic cells in the corneal epithelia at all ages, but the very small proportion of labeled cells precluded a quantitative analysis (data not shown). PH3$^+$ cells were noted in both wild-type and *PAX77*$^+$ corneal epithelia.

Cyclin E staining was used as a marker for cells around the G1/S transition. Staining was primarily localized to the nuclei of the basal epithelium, and the proportion of positive cells was counted as above, separately for central and peripheral cornea. No significant difference was found in the proportion of cyclin E$^+$ cells between the genotypes except in the peripheral cornea at P10, for which 73.7% ± 0.74 (n = 10) of *PAX77*$^+$ corneal epithelial cells were cyclin E$^+$, compared with 78.0% ± 0.688 (n = 10) of wild-types (Table 1). This may hint at problems with the cell cycle progression in the peripheral cornea at the critical stage of *PAX77*$^+$ corneal growth. Although highly significant (*t*-test: $P = 0.0001$), the difference is relatively small and restricted to peripheral cornea, so its biological significance may be minor.

p63 Is Expressed at Higher Frequency in the Basal Layer of the *PAX77*$^+$ Corneal Epithelium Than in Wild-type

P63 is a marker for stem-like cells and cells with high proliferative potential in the corneal epithelium (Pellegrini et al., 2002; Ramaesh et al., 2003; Senoo et al., 2007). Both eyes from four wild-type and four *PAX77*$^+$ adult mice and P10 and P2 neonates were investigated by p63 immunostaining. Within the corneal epithelium of both genotypes at all ages p63-positive nuclei were present in the basal layer. The distribution of p63-positive nuclei in the basal layer of the corneal epithelium was analyzed as for BrdU at all ages (Fig. 4C,D). There was no significant difference in the proportion of p63-expressing cells between peripheral

and central regions of either genotype at P2 (wild-type $P = 0.33$; *PAX77*$^{+}$ $P = 0.38$), P10 (wild-type $P = 0.68$; *PAX77*$^{+}$ $P = 0.099$), or in adults (wild-type $P = 0.0652$; *PAX77*$^{+}$ $P = 0.104$). The percentage of p63-positive cells was higher in *PAX77*$^{+}$ than wild-type in both peripheral and central regions of the cornea. This finding was not significant at P2 (*PAX77*$^{+}$ peripheral mean ± SEM 64.44 ± 5.02% vs. wild-type 54.17 ± 4.04%, $P = 0.129$ by unpaired *t*-test; *PAX77*$^{+}$ central mean ± SEM 70.36 ± 4.48% vs. 59.66 ± 3.64%, $P = 0.097$ by unpaired *t*-test) but became significant at P10 (*PAX77*$^{+}$ peripheral mean ± SEM 52.35 ± 3.17% vs. wild-type 43.17 ± 2.07%, $P < 0.05$ by unpaired *t*-test; *PAX77*$^{+}$ central mean ± SEM 59.38 ± 2.57% vs. wild-type 41.16 ± 4.25%, $P < 0.01$ by unpaired *t*-test) and in adults (*PAX77*$^{+}$peripheral mean ± SEM 58.38 ± 2.68% vs. wild-type 46.03 ± 2.1%, $P < 0.001$ by unpaired *t*-test; *PAX77*$^{+}$ central mean ± SEM 52.5 ± 2.68% vs. wild-type 37.09 ± 4.1%, $P < 0.01$ by unpaired *t*-test; Fig. 4).

No Abnormal Apoptosis in *PAX77*$^{+}$ Corneal Epithelia

We hypothesized that increased cell proliferation in the *PAX77*$^{+}$ corneal epithelium may be compensating for pathological apoptotic events secondary to increased Pax6 dosage. However, no Caspase-3 activity was noted by immunohistochemistry in corneal epithelia of either genotype at any age. The terminal deoxynucleotidyltransferase-mediated UTP end-labeling (TUNEL) labeling revealed apoptotic cells only in the superficial layer of the corneal epithelium in both genotypes, consistent with patterns of apoptosis only in desquamating cells as described previously (Ren and Wilson, 1996). No unusual apoptotic events were noted in *PAX77*$^{+}$ epithelia, and no difference was noted between the two genotypes (Fig. 4D).

K12 Expression Is Delayed and Reduced in *PAX77*$^{+}$ Corneal Epithelia

No defect in epithelial cells was noted by any of the four markers assaying different parameters of the cell cycle (above), and in fact, the results suggested that proliferation was higher in *PAX77*$^{+}$ than in wild-type. This finding recapitulates results obtained for *Pax6*$^{+/-}$ by Davis et al. (2003) and Ramaesh et al. (2005a). In *Pax6*$^{+/-}$ corneas, it was hypothesized that corneal fragility mediated by reduced cytokeratin-12 (K12) expression leads to increased cell desquamation and increases the proliferation rate in compensation (Davis et al., 2003). To determine K12 expression in *PAX77*$^{+}$ corneas, K12 immunohistochemical staining was performed on one eye of six adult mice and six 10-day-old neonates of each genotype. Levels of K12 expression were, on average, lower in *PAX77*$^{+}$ eyes than wild-type. As previously reported (Ramaesh et al., 2003, 2005a), the entire corneal epithelium of the wild-type eye is positive at all ages examined. K12 expression was much stronger in adult sections than at P10. The *PAX77*$^{+}$ eyes showed a range of different staining patterns in the corneal epithelium. In the central corneal epithelium of the adult *PAX77*$^{+}$ mice most sections showed positive staining, while some showed patchy staining, with few of the samples showing negative staining in the central regions. In *PAX77*$^{+}$ corneas, the central regions show more robust K12 expression when compared with peripheral regions at both P10 and in adults (Fig. 5A,B). By quantified Western blot, K12 expression in *PAX77*$^{+}$ corneas was on average 0.62× that in wild-type (n = 8 corneas, expression normalized against β-actin; Fig. 5C).

Wound Healing Is Delayed in *PAX77*$^{+}$ Corneal Epithelia

Circular epithelial wounds of diameter 0.8 mm were made in corneas of adult *PAX77*$^{+}$ mice, *Pax6*$^{+/-}$ mice, and their wild-type littermates, all on the same CBA/Ca genetic background. The rate of healing was measured as described in the Experimental Procedures section. Healing rates of both *Pax6*$^{+/-}$ and *PAX77*$^{+}$ epithelia were significantly slower than wild-type in control medium without serum or growth factors, and this retarded migration was maintained for 24 hr (Fig. 6).

We found that addition of 10% fetal calf serum to culture medium improved the rate of *Pax6*$^{+/-}$ corneal epithelium wound healing to 23.4 ± 3.01 μm/h, equivalent to wild-type (22.8 ± 4.56 μm/h), but had no significant effect on *PAX77*$^{+}$ corneas (15.7 ± 3.4 μm/h). Previously (Leiper et al., 2006), we showed that epidermal growth factor (EGF) could improve wound healing in *Pax6*$^{+/-}$ corneal epithelial cell monolayers in vitro by increasing the wound-induced waves of calcium and ERK1/2 signalling. Addition of 10 ng/ml EGF to the wound system described in this study (in absence of serum) also caused a significant increase in healing rates of *Pax6*$^{+/-}$ epithelia (Fig. 6A,B). In contrast, EGF was found to have no effect on wound healing rates of *PAX77*$^{+}$ corneas. Western blots were performed to assay levels of EGF-receptor (EGFR) in the *PAX77*$^{+}$ corneas, which was found to be 2.64-fold higher than wild-type (data normalized against β-actin expression, n = 2 blots of each genotype, each protein sample from four corneas; Fig. 6C). Failure of *PAX77*$^{+}$ corneas to respond to EGF was not, therefore, because the receptor was not expressed—EGFR levels rise in proportion to Pax6 dosage. A summary of all quantitative data is presented in Supplementary Table S1.

Defects in the *PAX77*$^{+}$ Lens

Transgenic overexpression of Pax6 isoforms in lens fibers has previously been shown to cause failure of normal lens fiber differentiation, leading to cataract (Duncan et al., 2000, 2004). The lens phenotype of the *PAX77*$^{+}$ model was also investigated. At the gross level, vacuoles were observed in lens from P2 (Fig. 7A,B), suggesting failure of lens fiber specification or elongation (n = 8). The lens bow region appeared normal, with nuclear localization of the transcription factor Prox1, which is required for fiber differentiation (Fig. 7C,D; Duncan et al., 2002). β-crystallins were expressed in lens fibers but not the lens epithelium (in a pattern identical to wild-type), and at the level of Western blot, although Pax6 was up-regulated compared with wild-type, β-crystallin isoforms were not down-regulated (Fig. 7E-G). Although the lens epithelium was grossly normal at P2, in adults, it became disrupted, with elongation to posterior regions of the lens and in some cases it was interrupted, with ectopic lens bows (Fig. 7H and Supplementary Figure S2). Consistent with partial failure of lens fiber differentiation, Pax6-positive cell nuclei were observed in the lens fiber region of all *PAX77*$^{+}$ lenses (n = 7); some nuclei from labeled animals were BrdU-positive, indicating active mitosis (Fig. 7I,J). No Pax6 or BrdU-positive nuclei were observed in any adult wild-type control lens.

DISCUSSION

What Controls Growth of the Cornea: *PAX77*$^{+}$ as a Mouse Model of Microcornea?

Little is known about the molecular or cellular control of corneal growth. In humans at birth, the cornea is approximately 90% of its adult diameter, and while the cornea reaches its final diameter by about the age of 3, the rest of the eye continues to grow for several more years (Oyster, 1999). We found that wild-type mouse corneas are less than 50% adult size at birth. In contrast, in *PAX77*$^{+}$ mice, while the corneal diameter is only slightly smaller than wild-type at birth, it subsequently fails to grow fully, and on average is already 90% of its final adult size (Fig. 2). Postnatal growth of the posterior segment of the *PAX77*$^{+}$ eye appears effectively normal in most cases, giving the mice a microcornea phenotype. This may suggest that the *PAX77*$^{+}$ mouse is a model of microcornea, but given that the dynamics of corneal growth in the *PAX77*$^{+}$ are similar to that seen in human, it may be better to regard wild-type mice more as a model of human megalocornea.

During the process of normal corneal growth, keratocytes produce regular arrays of collagen fibrils that constitute the bulk of the corneal stroma. A model of microcornea whereby keratocytes differentiate as normal but subsequently fail to produce normal quantities of

collagen (Oyster, 1999) would perhaps be consistent with the patterns of corneal growth failure seen in the *PAX77*$^{+}$ mice. However, corneal thickness has not been adversely affected in the *PAX77*$^{+}$, suggesting that any defect is restricted to tangential and radial collagen extension in the plane of the corneal circle. No such defect was observed by transmission electron microscopy in this study.

Although the data are equivocal, both total eye size and corneal diameter are at least in part modulated by intraocular pressure (IOP) during critical stages of growth (Coulombre, 1956, 1957; Neath et al., 1991; Schmid et al., 2003). IOP is in turn modulated by the secretory activity of the ciliary epithelium (Forrester et al., 2002), so there is a conceptual link between the morphological defects within the anterior eye and the microphthalmia/microcornea phenotypes in the mice.

K12—Delayed/Abnormal Differentiation

Previous results (Ramaesh et al., 2003, 2005a) showed that K12 is expressed throughout all cell layers of the wild-type corneal epithelium from 2 weeks after birth. Ramaesh et al. (2005a) noted that expression of K12 was delayed in *Pax6*$^{+/-}$ eyes, but improved with age. Unexpectedly, expression of K12 was also reduced in the *PAX77*$^{+}$ corneal epithelia compared with the wild-type, and there was some evidence of improvement with age (Fig. 5). In the *Pax6*$^{+/-}$ mouse, it was hypothesized that there was a decrease in K12 expression resulting in increased corneal fragility, which leads to increased cell loss and resulted in an increased cell proliferation rate to compensate (Davis et al., 2003). K12 deficiency has a disruptive effect on the structure of the corneal epithelium (Kao et al., 1996). In *K12*$^{-/-}$ mice, the number of keratin intermediate filaments in basal and suprabasal layers of the corneal epithelium is reduced and they appear as dense bundles rather than the normal fine filamentous networks that are normally seen (Kao et al., 1996). Also, the corneal epithelial layer becomes thinner and fragile, as a result corneal epithelial cells are unable to adhere firmly on to the corneal surface (Lu et al., 2001). This finding would suggest that K12 deficiency leads to a problem in corneal epithelial maintenance and a fragile corneal epithelium, which might underlie the increased cell proliferation seen in mice which both under- and overexpress Pax6.

Effect of Increased Pax6 Dosage on Cell Proliferation and Cell Cycle Progression

The cell cycle is driven by a family of cyclin-dependent protein kinases (CDKs), which are regulated in turn by cyclins whose synthesis, unlike the CDKs, is cell cycle-dependent (Draetta, 1991). There are four groups of cyclins: D, E, A, and B (Sherr, 1993). Expression of cyclin E, used in this study, is initiated in mid-G1 phase; maximal expression is occurs at the time of entry into S phase; and degradation occurs as the cell progresses through S phase (Sherr, 1993; Chung et al., 1999). Once cells have passed through the “restriction point” of G1 phase of the cell cycle, they are committed to pass through the remainder of the cell cycle (Chung et al., 1999); therefore, cells expressing cyclin E can be said to be actively progressing through the cell cycle.

None of the cell cycle assays we used, i.e., BrdU incorporation, cyclin E, and p63 expression, suggested any failure of cell cycling in *PAX77*$^{+}$ corneal epithelia in vivo. TUNEL labeling does not indicate a difference in cell loss through apoptosis between the two genotypes and, therefore, an increase in apoptosis probably does not account for the increase in proliferation that is seen in the *PAX77*$^{+}$.

In contrast, Ouyang et al. (2006) showed that Pax6 overexpression in vitro in a rabbit corneal epithelial cell line and rabbit primary cells retarded cell proliferation in a dose-dependent and cell autonomous manner, by blocking progression through the cell cycle.

Pax6 up-regulation also increased apoptosis up to fourfold by a Caspase-3-independent mechanism in that study. In this respect, it was perhaps surprising that we did not find any negative effect on proliferation in *PAX77*$^{+}$ corneal epithelia. However, the levels of Pax6 protein in adult *PAX77*$^{+}$ eyes were not as exaggerated as those promoted by the inducible system in Ouyang et al. (2006). Another source of variability between this study and that of Ouyang et al., is that, as Pinson et al. (2005) suggested, the relative ratios of the Pax6 and Pax6(+5a) isoforms may be as important to downstream gene regulation as the dosage of the gene per se. By Western blot, we found no significant difference between the endogenous Pax6:Pax6(5a) ratio and that in the *PAX77*$^{+}$ mouse, but this was not the case for the inducible system described by Ouyang et al. (2006), in which only one isoform was overexpressed. The differences may also reflect the additional complexity of the in vivo situation (with cell loss, tissue-tissue interactions modulated by a variable environment) over the in vitro cell monolayer system, which serves a different purpose in examining only the autonomous effects of Pax6 overexpression in a controlled simple system. It would appear that the corneal epithelium is maintained in the *PAX77*$^{+}$ mouse in a regulated system that acts despite the autonomous tendencies of Pax6 to retard the cell cycle and promote apoptosis in epithelial cells.

It was considered possible that, because the lens acts as an organizer of anterior segment development and has previously been shown to be particularly sensitive to Pax6 dosage, the corneal phenotype observed in *PAX77*$^{+}$ may be a secondary consequence of increased dosage of Pax6 in the lens (Coulombre and Coulombre, 1964; Thut et al., 2001; Collinson et al., 2001). However, previous models of lens-specific Pax6 isoform overexpression (Duncan et al., 2000, 2004) did not report microcornea, suggesting that corneal Pax6 dosage is the primary cause of the corneal phenotype seen here. The lens phenotype reported in this study, at P2 (hence before the onset of the corneal phenotype), is superficially similar to that reported in Duncan et al. (2000, 2004).

Wound Healing in *PAX77*$^{+}$ Mice

We found that both *Pax6*$^{+/-}$ and *PAX77*$^{+}$ corneal epithelia heal more slowly than wild-type in ex vivo whole eye organ culture in defined medium without serum. Addition of fetal calf serum to *Pax6*$^{+/-}$ corneal epithelia ex vivo cultures dramatically increased the rate of wound healing to at least wild-type levels (comparable to results obtained previously for *Pax6*$^{+/-}$ corneal epithelia by Ramaesh et al. [2006] in serum-supplemented medium) but did not affect wild-types or *PAX77*$^{+}$ corneas. These data are interesting for several reasons. First, it appears that wild-type eyes are self-sufficient for all the cytokines and growth factors required to maintain wound healing, in the absence of continuing vascular and nervous supply, such that addition of exogenous serum does not improve corneal performance. Second, that *Pax6*$^{+/-}$ are deficient in at least one of these cytokines and growth factors, but are capable of migrating at wild-type levels if serum is applied exogenously. In this study, we found that addition of EGF alone did not affect wild-type corneas, but corrected the wound healing rate *Pax6*$^{+/-}$, consistent with our previous work on murine corneal epithelial monolayers (Leiper et al., 1996) and suggesting that modulation of the EGF signalling pathway may offer a therapeutic strategy for the corneas of aniridic patients. Third, although *PAX77*$^{+}$ corneal epithelia are also deficient in wound healing in serum-free medium, a superficial similarity with *Pax6*$^{+/-}$, the deficiency is not related to lack of growth factors, because addition of serum or EGF to defined medium does not increase the rate of *PAX77*$^{+}$ cell migration.

Previously we suggested that failure of prompt wound healing in *Pax6*$^{+/-}$ mice might underlie long-term degeneration leading to opacity (Leiper et al., 1996), and we have shown in two systems (corneal epithelial cell monolayers and whole eye culture) that *Pax6*$^{+/-}$ cells

show a delayed wounding response. However, the *PAX77*$^{+}$ mice suggest that corneal transparency can be maintained despite very severe wound healing defects.

Similarities and Differences Between *PAX77*$^{+}$ and *Pax6*$^{+/-}$

Previous work emphasized the similarity between the phenotype of *Pax6*$^{+/-}$ and *PAX77*$^{+}$ mice, suggesting that both over- and underexpression of Pax6 led to equivalent eye abnormalities. We have now more explicitly compared the eyes of these two strains, summarized in Table 2, and at the molecular level there are some surprising similarities. Cell proliferation is increased in both *Pax6*$^{+/-}$ and *PAX77*$^{+}$, and expression of cytokeratin-12 was reduced in both. While proliferation rate is a function of a balance between multiple factors affecting cell loss and stem cell activity, potentially several steps downstream of direct Pax6 target genes, the reduction of cytokeratin-12 expression in *Pax6*$^{+/-}$ and *PAX77*$^{+}$ corneas is unexpected because K12 is reported to be a direct transcriptional target of Pax6 (Liu et al., 1999). In microarray analysis of the lens (Chauhan et al., 2002b), proportionately few of the identified Pax6 downstream genes were both down-regulated in *Pax6*$^{+/-}$ and up-regulated in Pax6 overexpressing lenses, suggesting that gene transcription profiles in tissues with different Pax6 dosages are neither simple nor intuitive.

EXPERIMENTAL PROCEDURES

Mice

PAX77^{+} transgenics were maintained on the CBA/Ca genetic background (known as "*CBA77*"), breeding *PAX77*$^{+}$ × "wild-type" *PAX77*$^{-}$ CBA/Ca to produce hemizygous *PAX77*$^{+}$ and wild-type littermates. *PAX77*$^{+}$ mice were identified by their eye size and their genotype confirmed by polymerase chain reaction (PCR). Mice were killed by cervical dislocation, and the eyes were immediately removed and fixed in 4% paraformaldehyde (PFA) or the eyes were immediately wounded and then removed for culturing. For BrdU labeling experiments, mice of mass 25-32 g were injected with 0.2 ml of 10 mg/ml BrdU in saline 4 hr before death. Adult mice in this study were taken at 8-15 weeks old.

Histological Analysis

Eyes were fixed in 4% PFA for 2 hr, then processed to wax, and 7-μm sections were cut. Eyes were sectioned in an anterior-posterior plane to include cornea, lens, and retina. Histological features of the cornea of *PAX77*$^{+}$ and wild-type littermates at P2, P10, and adult were then compared. For PAS staining, slides were treated with periodic acid, 15 min, washed, and stained with Schiff's reagent, 5 min.

Morphometric Measurements

Corneal diameter was measured in *PAX77*$^{+}$ and wild-type P2, P10, and adult eyes using a stereomicroscope. Tissue sections of adult cornea were viewed under a light microscope (×40 objective), and measurements were made using a calibrated eyepiece graticule. The thickness of the corneal epithelium and the whole cornea were measured in three places (two peripheral regions and one central) in 5 of the middle 13 serial sections of each eye (mid - 6, mid - 3, midsection, mid + 3, mid + 6). Mean thicknesses were calculated for both the central and peripheral cornea. The number of cell layers in the corneal epithelium was also counted in the same sections allowing the mean cell layers for each eye to be calculated.

Immunohistochemical Staining

Deparaffinized sections were washed in 100% ethanol, incubated with 3% hydrogen peroxide, 20 min, in methanol, to block endogenous peroxidase activity, re-hydrated with 70% ethanol and washed with phosphate buffered saline (PBS). Antigen retrieval was

performed by boiling in 0.01 M citrate buffer, pH 6, 20 min. Slides were washed with Tris-buffered saline (TBS: 100 mM Tris, 0.9% NaCl, pH7.6) and blocked with 4% normal serum (species according to secondary antibody) in TBS, 0.3% bovine serum albumen, 2 hr at room temperature. Primary antibody incubation overnight at 4°C (P63: Santa Cruz sc-8431 diluted 1:200; Pax6: Developmental Studies Hybridoma Bank, University of Iowa diluted 1:500; BrdU: BD Biosciences 347580, diluted 1:200; cyclin E: Santa Cruz sc-481, diluted 1:200; K12: Santa Cruz sc-17101, diluted 1:400; Prox1: Sigma P7124, diluted 1:300; β-crystallin Santa Cruz sc-22745, diluted 1:100). Slides were washed in TBS and then treated with the secondary antibody (P63, Pax6, and BrdU: Dakocytomation UK Ltd, biotinylated rabbit anti-mouse IgG diluted 1:200 in blocking buffer; cyclin E: Sigma biotinylated goat anti-rabbit IgG; K12: Invitrogen Alexa 488 donkey anti-rabbit A21206 or Alexa 488 goat anti-mouse IgG1 A21121 diluted 1:500 in blocking buffer) for 45 min then washed in TBS. All slides for which a nonfluorescent secondary was used were treated with avidin-biotin complex (ABC; Dakocytomation UK Ltd) for 30 min washed with TBS and 20mM Tris pH 7.5. The binding antibody was then visualized by 3,3′-diaminobenzidine (DAB) stain (5.9 ml of 20 mM Tris pH 7.6, 100 μl of 50 mg/ml DAB, 1 μl of H_2O_2). Control slides were treated with normal blocking buffer without primary antibody, but otherwise treated normally. Fluorescence immunohistochemistry was quantified by grabbing individual nuclei from wild-type and *PAX77*$^+$ sections processed in parallel and immunostained on the same slides, and measuring their luminosity in Adobe Photoshop7.

Analysis of P63, cyclin E, and K12 Expression Patterns and BrdU Incorporation

For quantitative analysis of P63, cyclin E, and BrdU, each cell in the basal cell layer was scored as either positive or negative along the entire length of the corneal epithelium. Fully intact corneal sections from central serial sections were scored. Mid regions of the cornea were split into four equal sections with the outer sectors representing the peripheral cornea and inner sectors the central cornea (Fig. 4). The distribution of P63, cyclin E, and BrdU was calculated separately for the peripheral and central corneal in both *PAX77*$^+$ and wild-type littermates.

K12 expression was scored separately in the peripheral and central cornea in PAX77 mutants and wild-type mice at various ages. Ten serial sections obtained from the middle of each eye were scored for K12 staining pattern as positive, negative, or “patchy” similar to the scoring system in Ramaesh et al. (2005a). For descriptive purposes, positive epithelia were defined when all cells exhibited staining throughout the epithelium above background of labeling by normal rabbit serum. Negative staining indicated background only. In patchy stained epithelium, staining was heterogeneous, with some cells clearly positive and others at or around background levels.

Apoptosis

The TUNEL in situ cell death detection kit, fluorescein (Roche Diagnostics) was used to label apoptotic cells in the corneal epithelium of tissue sections. Dewaxed sections were exposed to proteinase K (80 μg/ml) for 5 min at room temperature. Slides were washed three times in PBS. One slide was treated with DNAse1 as a positive control (50 units/ml DNAse1 in 50 mM Tris-HCl pH 7.5, 1 mM MgCl 1 mg/ml BSA for 30 min at 37°C, followed by three 5-min washes in PBS). TUNEL labeling was then performed per the manufacturer’s instructions. Slides were then washed three times for 5 min in PBS and mounted in Vectashield (VectorLabs, UK).

Western Blot Analysis

Whole corneas were dissected from the eyes into lysis buffer. The cornea was subjected to 10% sodium dodecyl sulfate-polyacrylamide gel elecrophoresis, and transferred to a

nitrocellulose membrane. After blocking, the blots were incubated with primary antibody (anti-mouse Pax6 monoclonal antibody [1:2,000] or total EGFR monoclonal antibody [1:1,000] overnight at 4°C), washed, and then treated with the secondary antibody anti mouse IgG horseradish peroxidase (1:3,000) for 1 hr at room temperature. The blot was then washed and visualized by the ECL system according to the manufacturer's instructions.

Corneal Epithelial Wound Healing

A trephine blade of diameter 0.8 mm was used to introduce a wound in the center of the cornea, under a dissecting microscope. An ophthalmological scalpel was used to de-bride the corneal epithelium within the wound. The wound area in both *PAX77*$^{+}$ and *PAX77*$^{-}$ mice was visualized by topical application of sodium fluorescein and photographed with a digital camera on a dissecting microscope. The eyes was then enucleated and placed into a culture wells (corneas facing up) containing Keratinocyte Basal Medium (Cambrex, UK), DMEM/HAM F-12, 25 mM HEPES buffer, 125 μg/ml gentamycin and 125 μM 2-β-ME (Hazlett et al., 1996). Unless otherwise stated, the culture medium contained no fetal bovine serum. To determine the role of EGF in modulating wound healing, 10 ng/ml murine EGF (Sigma, Poole, UK) was added. Eyes were maintained at 37°C in 5% CO_2 and allowed to heal with the wound area being visualized and photographed at set time points. Reduction in wound area was observed over time and continued for over 24 hr under these conditions. The change in wound diameter over time was measured and calculated using Adobe Photoshop Pro.

Statistical Analysis

Unpaired *t*-tests were used to compare results obtained in the *PAX77*$^{+}$ and wild-type littermates.

Supplementary Material

Refer to Web version on PubMed Central for supplementary material.

Acknowledgments

N.D. is funded by a Biotechnology and Biological Sciences Research Council DTI PhD studentship, and work in JMC's laboratory is funded by Wellcome Trust project grant 074127 (RK, JMC) and BBSRC research grant BB/E015840/1 (JO, JMC). IP is funded by a James Mearns Trust PhD studentship at University of Aberdeen. RK was funded by a University of Aberdeen College PhD. Studentship.

REFERENCES

Aalfs CM, Fantes JA, Wenniger-Prick LJ, Sluijter S, Hennekam RC, van Heyningen V. Tandem duplication of 11p12-p13 in a child with borderline development delay and eye abnormalities: dose effect of the PAX6 gene product. Am J Med Genet. 1997; 73:267–271. [PubMed: 9415682]

Baulmann DC, Ohlmann A, Flugel-Koch C, Goswami S, Cvekl A, Tamm ER. Pax6 heterozygous eyes show defects in chamber angle differentiation that are associated with a wide spectrum of other anterior eye segment abnormalities. Mech Dev. 2002; 118:3–17. [PubMed: 12351165]

Chao LY, Huff V, Strong LC, Saunders GF. Mutation in the PAX6 gene in twenty patients with aniridia. Hum Mutat. 2000; 15:332–339. [PubMed: 10737978]

Chauhan BK, Reed NA, Zhang W, Duncan MK, Kilimann MW, Cvekl A. Identification of genes downstream of Pax6 in the mouse lens using cDNA microarrays. J Biol Chem. 2002a; 277:11539–11548. [PubMed: 11790784]

Chauhan BK, Reed NA, Yang Y, Cermak L, Reneker L, Duncan MK, Cvekl A. A comparative cDNA microarray analysis reveals a spectrum of genes regulated by *Pax6* in mouse lens. Genes to Cells. 2002b; 7:1267–1283. [PubMed: 12485166]

Chung EH, Hutcheon AEK, Joyce CN, Zieske JD. Syncronization of the G1/S transition in response to corneal debridement. Invest Ophthalmol Vis Sci. 1999; 40:1952–1958. [PubMed: 10440248]

Churchill AJ, Hanson IM, Markham AF. Prenatal diagnosis of aniridia. Ophthalmology. 2000; 107:1153–1156. [PubMed: 10857836]

Collinson JM, Quinn JC, Buchanan MA, Wedden SE, Kaufman MH, West JD, Hill RE. Primary defects in the lens underlie complex anterior segment abnormalities in the *Pax6* heterozygous eye. Proc Natl Acad Sci U S A. 2001; 98:9688–9693. [PubMed: 11481423]

Collinson JM, Morris L, Reid AI, Ramaesh T, Keighren MA, Flockhart JH, Hill RE, Tan S-S, Ramaesh K, Dhillon B, West JD. Clonal analysis of patterns of growth, stem cell activity and cell movement during the development and maintenance of the murine corneal epithelium. Dev Dyn. 2002; 224:432–440. [PubMed: 12203735]

Collinson JM, Chanas SA, Hill RE, West JD. Corneal development, limbal stem cell function, and corneal epithelial cell migration in the *Pax6*$^{+/-}$ mouse. Invest Ophthalmol Vis Sci. 2004; 45:1101–1108. [PubMed: 15037575]

Cotsarelis G, Cheng S-Z, Dong G, Sun T-T, Lavker RM. Existence of slow-cycling limbal epithelial basal cells that can be preferentially stimulated to proliferate: implications on epithelial stem cells. Cell. 1996; 57:201–209. [PubMed: 2702690]

Coulombre AJ. The role of intraocular pressure in the development of the chick eye. I. Control of eye size. J Exp Zool. 1956; 133:211–215.

Coulombre AJ. The role of intraocular pressure in the development of the chick eye. II. Control of corneal size. Arch Ophthalmol. 1957; 57:250–254.

Coulombre AJ, Coulombre JL. Lens development. I. Role of the lens in eye growth. J Exp Zool. 1964; 156:39–42. [PubMed: 14189921]

Davis J, Duncan MK, Robison WG Jr, Piatigorsky J. Requirement for Pax6 in corneal morphogenesis: a role in adhesion. J Cell Sci. 2003; 116:2157–2167. [PubMed: 12692153]

Draetta G. A series of reviews on the biochemistry and biology of Cdc2/28-cyclin complexes. Semin Cell Biol. 1991; 2:193–271.

Duncan MK, Kozmik Z, Cveklova K, Piatigorsky J, Cvekl A. Overexpression of PAX6(5a) in lens fiber cells results in cataract and upregulation of (alpha)5(beta)1 integrin expression. J Cell Sci. 2000; 113:3173–3185. [PubMed: 10954416]

Duncan MK, Cui W, Oh DJ, Tomareu I. Proxl is differentially localized during lens development. Mech Dev. 2002; 112:195–198. [PubMed: 11850194]

Duncan MK, Xie L, David LL, Robinson ML, Taube JR, Chi W, Reneker LW. Ectopic Pax6 expression disturbs lens fiber cell differentiation. Invest Ophthalmol Vis Sci. 2004; 45:3589–3598. [PubMed: 15452066]

Epstein J, Cai J, Glaser T, Jepeal L, Maas R. Identification of a Pax paired domain recognition sequence and evidence for DNA-dependent conformational changes. J Biol Chem. 1994; 269:8355–8361. [PubMed: 8132558]

Forrester, JV.; Dick, AD.; Mcmenamin, PG.; Lee, WR. The eye: basic sciences in practice. Edinburgh: Saunders; 2002.

Grindley JC, Davidson DR, Hill RE. The role of Pax-6 in eye and nasal development. Development. 1995; 121:1433–1442. [PubMed: 7789273]

Hazlett L, Masinick S, Mezger B, Barrell R, Kurpakus M, Garrett M. Ultrastructural, immunohistological and biochemical characterization of cultured mouse corneal epithelial cells. Ophthalmic Res. 1996; 28:50–56. [PubMed: 8726677]

Hill RE, Favor J, Hogan BLM, Ton CCT, Saunders GF, Hanson IM, Prosser J, Jordan T, Hastie ND, van Heyningen V. Mouse *Small eye* results from mutations in a *paired*-like homeobox-containing gene. Nature. 1991; 354:522–525. [PubMed: 1684639]

Holland EJ, Djalilian AR, Schwartz GS. Management of aniridic keratopathy with keratolimbal allograft: a limbal stem cell transplantation technique. Ophthalmology. 2003; 110:125–130. [PubMed: 12511357]

Kao WW, Liu CY, Converse RL, Shiraishi A, Kao CW, Ishizaki M, Doetschman T, Duffy J. Keratin 12-deficient mice have fragile corneal epithelia. Invest Ophthalmol Vis Sci. 1996; 37:2572–2584. [PubMed: 8977471]

Europe PMC Funders Author Manuscripts

Koroma BM, Yang J, Sundin OH. The *Pax-6* homeobox gene is expressed throughout the corneal and conjunctival epithelia. Invest Ophthalmol Vis Sci. 1997; 38:108–120. [PubMed: 9008636]

Kucerova R, Ou J, Leiper LJ, Collinson JM. Cell surface glycoconjugate abnormalities and corneal epithelial wound healing in the pax6+/- mouse model of aniridia-related keratopathy. Invest Ophthalmol Vis Sci. 2006; 47:5276–5282. [PubMed: 17122113]

Leiper LJ, Walczysko P, Kucerova R, Ou J, Shanley LJ, Lawson D, Forrester JV, McCraig CD, Zhao M, Collinson JM. The roles of calcium signaling and ERK1/2 phosphorylation in a *Pax6*$^{+/-}$ mouse model of epithelial wound-healing delay. BMC Biol. 2006; 4:27. [PubMed: 16914058]

Liu JJ, Kao WW-Y, Wilson SE. Corneal epithelium-specific mouse keratin K12 promoter. Exp Eye Res. 1999; 68:295–301. [PubMed: 10079137]

Lu L, Reinach PS, Kao WW. Corneal epithelial wound healing. Exp Biol Med. 2001; 226:653–664.

Neath P, Roche SM, Bee JA. Introcular pressure-dependent and independent phases of growth of the embryonic chick eye and cornea. Invest Ophthalmol Vis Sci. 1991; 32:2483–2491. [PubMed: 1869402]

Nelson LB, Spaeth GL, Nowinski TS, Margo CE, Jackson L. Aniridia a review. Surv Ophthalmol. 1984; 28:621–642. [PubMed: 6330922]

Nishida K, Kinoshita S, Ohashi Y, Kuwayama Y, Yamamoto S. Ocular surface abnormalities in aniridia. Am J Ophthalmol. 1995; 120:368–375. [PubMed: 7661209]

Ouyang J, Shen Y-C, Yeh L-K, Li W, Liu CY, Fini E. *Pax6* overexpression suppresses cell proliferation and retards the cell cycle in corneal epithelial cells. Invest Ophthalmol Vis Sci. 2006; 47:2397–2407. [PubMed: 16723449]

Oyster, CW. The human eye. Sunderland, MA: Sinauer; 1999.

Pellegrini G, Dallembra E, Golisano O, Martinelli E, Fantozzi I, Bondanza S, Ponzin D, McKeon F, De Luca M. p63 identifies keratinocyte stem cells. Proc Natl Acad Sci (USA). 2001; 98:3156–3161. [PubMed: 11248048]

Pinson J, Simpson TI, Mason JO, Price DJ. Regulation of the Pax6: Pax6(5a) mRNA ratio in the developing mammalian brain. BMC Dev Biol. 2005; 5:13. [PubMed: 16029501]

Ramaesh J, Collinson JM, Ramaesh K, Kaufman MH, West JD, Dhillon B. Corneal abnormalities in *Pax6*$^{+/-}$ small eye mice mimic human aniridia-related keratopathy. Invest Ophthalmol Vis Sci. 2003; 44:1871–1878. [PubMed: 12714618]

Ramaesh T, Ramaesh K, Collinson JM, Chanas S, Dhillon B, West JD. Developmental and cellular factors underlying corneal epithelial dysgenesis in the *Pax6*$^{+/-}$ mouse model of aniridia. Exp Eye Res. 2005a; 81:224–235. [PubMed: 16080917]

Ramaesh K, Ramaesh T, Dutton GN, Dhillon B. Evolving concepts on the pathogenic mechanisms of aniridia related keratopathy. Int J Biochem Cell Biol. 2005b; 37:547–557. [PubMed: 15618012]

Ramaesh T, Ramaesh K, Leask R, Springbett A, Riley S, Dhillon B, West JD. Increased apoptosis and abnormal wound-healing responses in the heterozygous *Pax6*$^{+/-}$ mouse cornea. Invest Ophthalmol Vis Sci. 2006; 47:1911–1917. [PubMed: 16638998]

Ren H, Wilson G. Apoptosis in the corneal epithelium. Invest Ophthalmol Vis Sci. 1996; 37:1017–1025. [PubMed: 8631617]

Schedl A, Ross A, Lee M, EngelKamp D, Rashbass P, van Heyningen V, Hastie ND. Influence of PAX6 gene dosage on development: overexpression causes severe eye abnormalities. Cell. 1996; 86:71–82. [PubMed: 8689689]

Schmid KL, Hills T, Abbott M, Humphries M, Pyne K, Wildsoet CF. Relationship between intraocular pressure and eye growth in the chick. Ophthal Physiol Opt. 2003; 23:25–33.

Senoo M, Pinto F, Crum CP, McKeon F. p63 is essential for proliferative potential of stem cells in stratified epithelia. Cell. 2007; 129:523–536. [PubMed: 17482546]

Shaw HA. Ocular therapeutics in general practice. Lancet. 1960; 80:359–365.

Sherr CJ. Mammalian G1 genes. Cell. 1993; 73:1059–1065. [PubMed: 8513492]

Sivak JM, Mohan R, Rinehart WB, Xu PX, Maas RL, Fine ME. Pax-6 expression and activity in the reepithelialising cornea control activity of the transcriptional promoter for matrix metalloproteinase gelatinase B. Dev Biol. 2002; 222:41–54. [PubMed: 10885745]

Sivak JM, West-Mays JA, Yee A, Williams T, Fini ME. Transcription factors Pax6 and AP-2alpha interact to coordinate corneal epithelial repair by controlling expression of matrix metalloproteinase Gelatinase B. Mol Cell Biol. 2004; 24:245–257. [PubMed: 14673159]

Thut CJ, Rountree RB, Hwa M, Kingsley DM. A large-scale in situ screen provides molecular evidence for the induction of eye anterior segment structures by the developing lens. Dev Biol. 2001; 231:63–76. [PubMed: 11180952]

Ton CC, Hirvonen H, Miwa H, Weil MN, Monaghan P, Jordan T, van Heyningen V, Hastie ND, Meijers-Heijboer H, Drecgsler M. Positional cloning and characterization of a paired box- and homeobox-containing gene from the aniridia region. Cell. 1991; 67:1059–1074. [PubMed: 1684738]

Europe PMC Funders Author Manuscripts

Europe PMC Funders Author Manuscripts

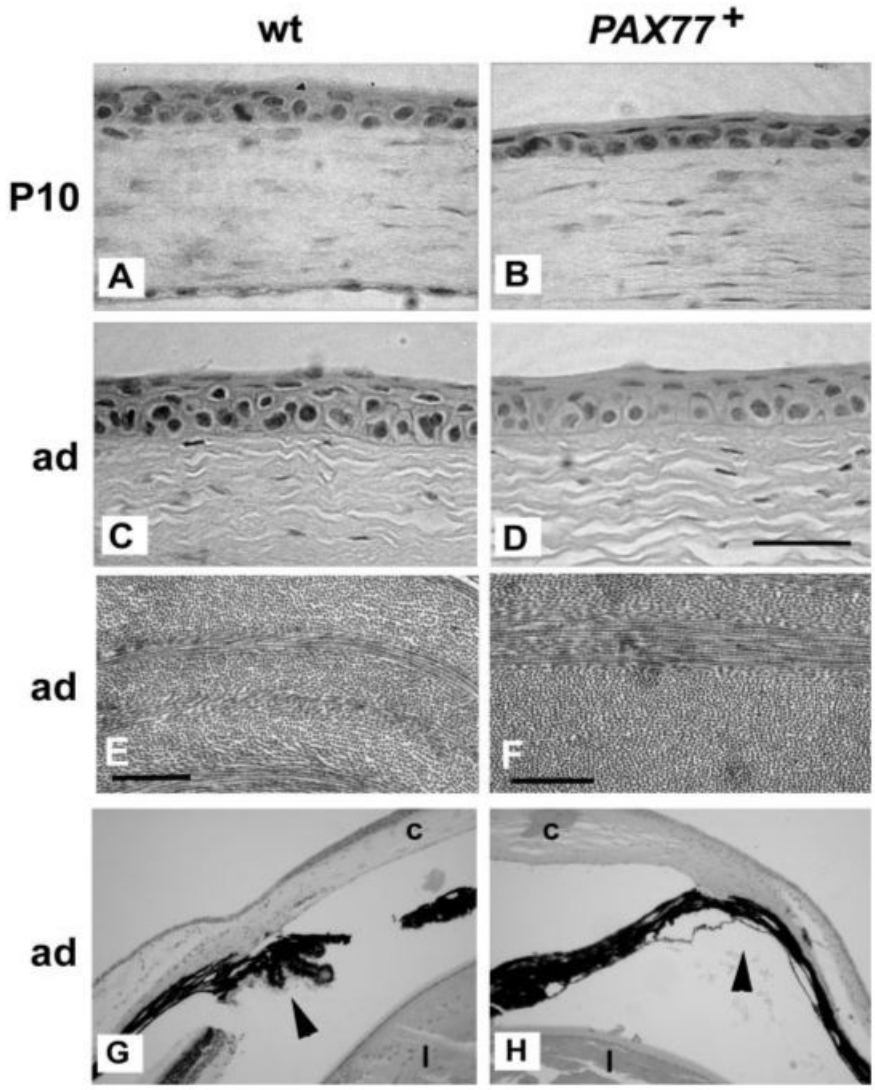

Fig. 1.

Histological analysis of the anterior segment of the eye of the *PAX77*$^{+}$ transgenic mice. **A,B:** Comparison of the corneas of postnatal day (P) 10 wild-type (A) shows the corneal epithelium is stratified and is made up of two to three cell layers; the same pattern is seen in the *PAX77*$^{+}$ (B). **C,D:** In the adult comparison of the corneal sections of both wild-type (C) and *PAX77*$^{+}$ (D) revealed that the *PAX77*$^{+}$ corneal epithelium was relatively normal. Quantitative analysis (see text) showed that, on average, it was composed of fewer cell layers than wild-type. **E,F:** Transmission electron microscope image of corneal stroma of wild-type (E) and *PAX77*$^{+}$ (F) corneal stroma, showing that the interfibrillary gaps in (C) and (D) are processing artifacts and that collagen fiber lamination is normal in *PAX77*$^{+}$. **G:** A normal ciliary body seen in the adult wild-type (arrowhead). **H:** Lack of a ciliary body (arrowhead) and iris hyperplasia in the *PAX77*$^{+}$. l, lens; c, cornea. Scale bar = 50 μm in A-D, 2 μm in E,F.

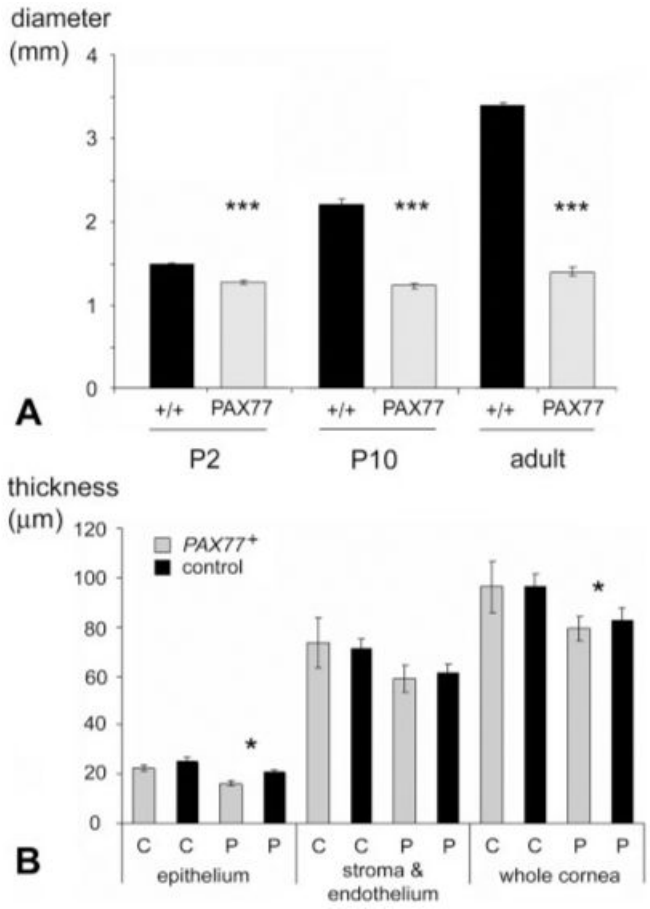

Fig. 2.

Corneal morphometry. **A:** Comparison of cornea diameter (mm) in *PAX77*$^{+}$ and wild-types age postnatal day (P) 2, P10, and adult. **B:** Comparison of thickness of central (C) and peripheral (P) regions of the cornea in adult *PAX77*$^{+}$ and wild-type mice. *$P < 0.01$, ***$P <$ 0.0001 by unpaired *t*-test.

Europe PMC Funders Author Manuscripts

Europe PMC Funders Author Manuscripts

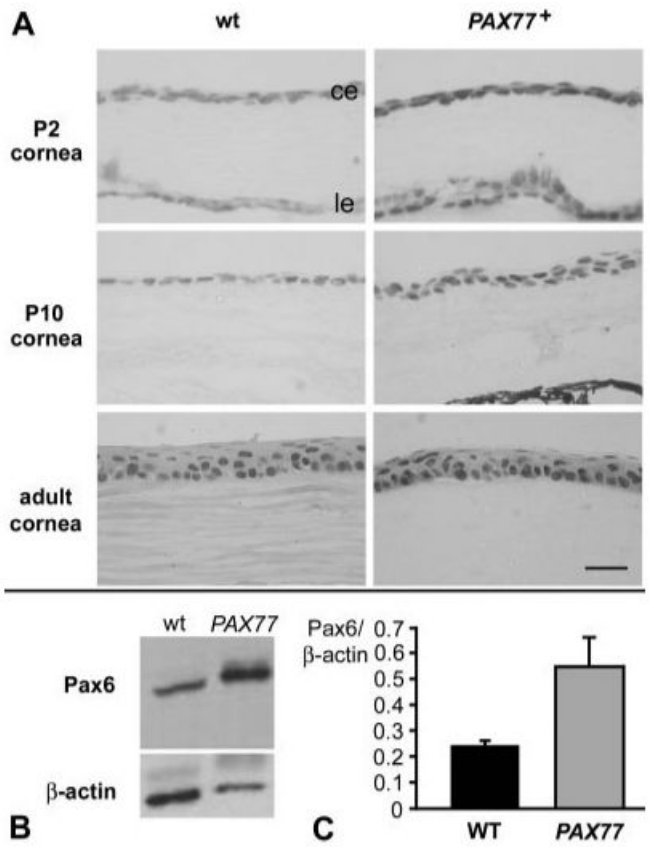

Fig. 3.

Pax6 expression. **A:** Pax6 immunohistochemical staining in *PAX77*$^{+}$ and wild-type eyes at postnatal day (P) 2, P10, and in adults. Pax6 expression in the cornea is increased in the *PAX77*$^{+}$ at postnatal day 2 and postnatal day 10. **B,C:** Increased Pax6 expression in the cornea of the *PAX77*$^{+}$ adults was confirmed by Western blot, and shown to be statistically significant when quantified and normalized against β-actin expression (C). Scale bar = 30 μm.

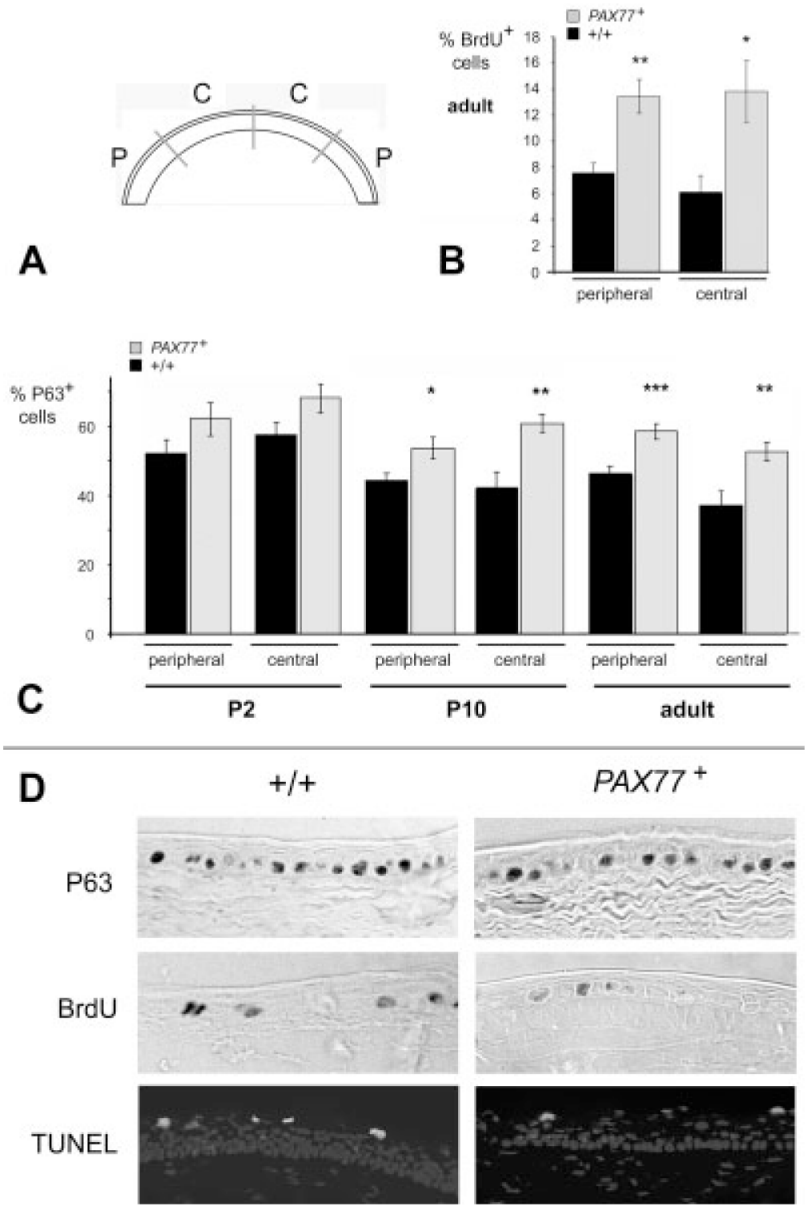

Fig. 4.

Corneal epithelial proliferation. **A,B:** Frequency of bromodeoxyuridine (BrdU) -positive cells in the basal layer of the corneal epithelium in central and peripheral regions of the cornea in adult wild-type and *PAX77*$^{+}$ mice. **C:** Distribution of p63-expressing cells in the peripheral and central cornea of the basal layer of the corneal epithelium of wild-type and *PAX77*$^{+}$ eyes in adults and postnatal day (P) 10 and P2 neonates. **D:** Immunohistochemical staining to visualize p63-positive cells in the wild-type corneal epithelium. Immunohistochemical staining to identify proliferating cells in the wild-type corneal epithelium that have incorporated BrdU. Terminal deoxynucleotidyltransferase-mediated UTP end-labelling (TUNEL) labeling (green) of apoptotic cells in the superficial layers of the wild-type and *PAX77*$^{+}$ corneal epithelium. 4′,6-diamidine-2-phenylidole-dihydrochloride (DAPI) nuclear counterstain is visible.

Europe PMC Funders Author Manuscripts

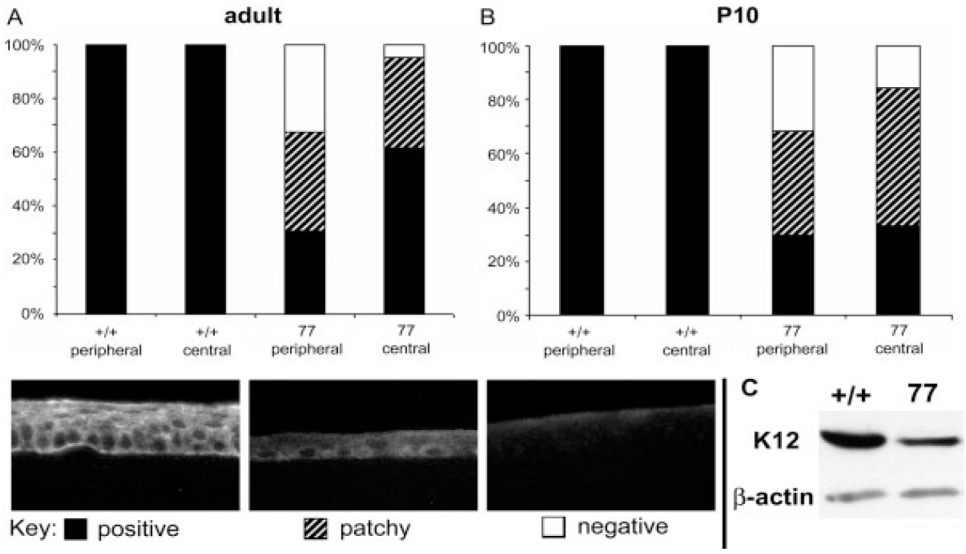

Fig. 5.

Cytokeratin-12 expression. **A,B:** Bar charts grouping samples by K12 expression in both peripheral and central regions of the cornea in both wild-type and *PAX77*$^{+}$ mice in adults (A) and postnatal day 10 (B). Bars are divided to represent the frequency of positive, patchy, and negatively stained samples. **C:** Western blot of K12 expression in wild-type and PAX77^{+} corneas.

Europe PMC Funders Author Manuscripts

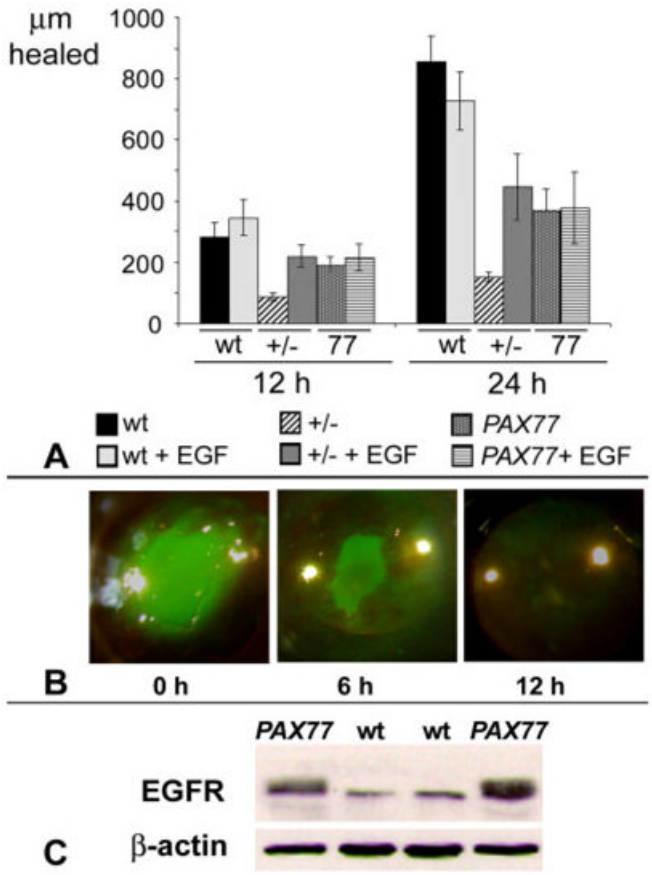

Fig. 6.

Wound healing. **A:** Histogram showing change in wound diameter (i.e., amount of healing) at 12 and 24 hr after wounding, in wild-type, *Pax6*$^{+/-}$, and *PAX77*$^{+}$ eyes cultured in serum-free culture medium ± 10 ng/ml epidermal growth factor (EGF). **B:** Representative images of a single wild-type eye immediately after wounding and 6 hr and 12 hr after wounding, showing complete closure of the wound after 12 hr. The wounds were topically stained with fluorescein to visualize the wound area. **C:** Western blot analysis of EGF receptor (EGFR) expression in wild-type and PAX77 whole cornea, showing increased expression of EGFR in the *PAX77*$^{+}$. Each lane was pooled from four separate corneas.

Europe PMC Funders Author Manuscripts

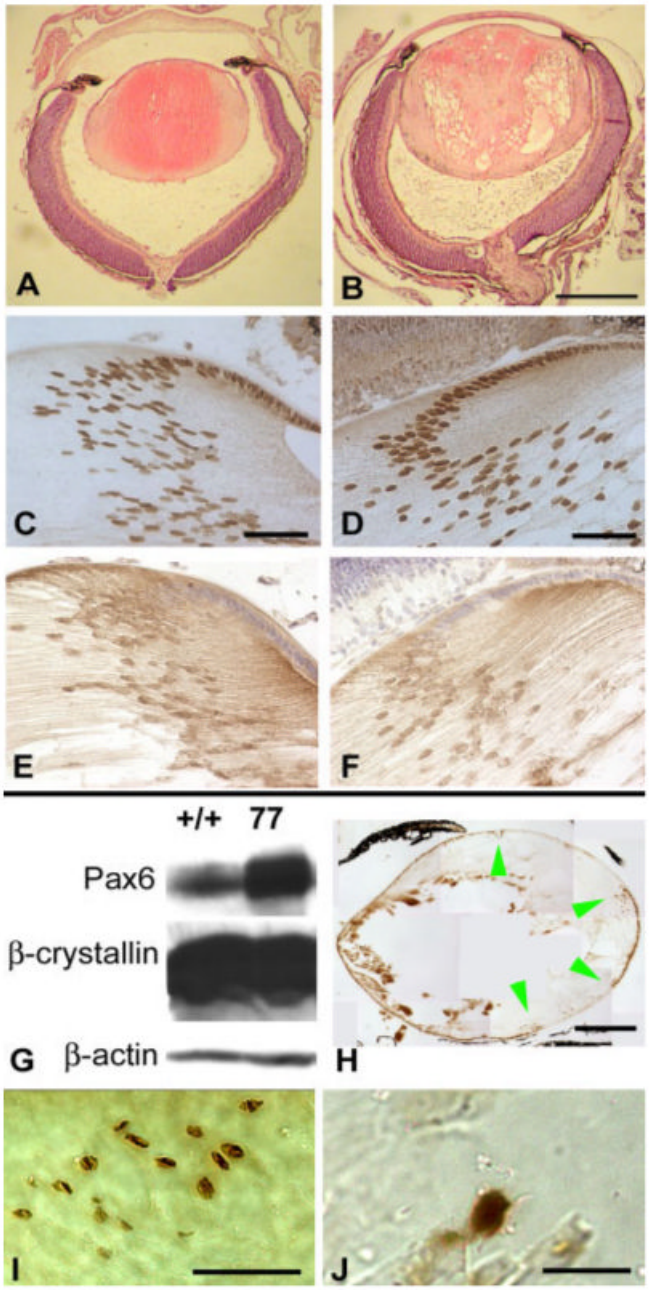

Fig. 7.

Lens defects. **A-F:** Histology of postnatal day (P) 2 wild-type (A,C,E) and *PAX77*$^{+}$ (B,D,F) lenses, with hematoxylin and eosin staining (A,B), anti-Prox1 immunohistochemistry (C, D), and anti-β-crystallin (E,F). **G:** Western blot analysis of Pax6 and β-crystallins in the *PAX77*$^{+}$ lens. **H:** Lens epithelial dysgenesis in a *PAX77*$^{+}$ lens. Top of image is anterior. Green arrowheads represent lens bows of displaced and fragmented epithelium. A composite high-resolution image is presented as Supplementary Figure 2. **I,J:** Ectopic nuclei in adult *PAX77*$^{+}$ lens fiber region are Pax6-positive (I) and, with low frequency, BrdU-positive. Scale bars = 500 μm in A,B, 50 μm in C,D, 320 μm in H, 50 μm in I, 10 μm in J.

Europe PMC Funders Author Manuscripts

TABLE 1

Percentage of Cells Expressing Cyclin E in the *PAX77*$^{+}$ Corneal Epithelium

	Percentage cyclin E expression				*P* values	
Region of cornea	**Peripheral cornea**		**Central cornea**			
Genotype Mouse age	**PAX77**	**Wild-type**	**PAX77**	**Wild-type**	**Peripheral**	**Central**
Adult	75.6	76.5	75.6	74.9	0.33	0.77
Postnatal day 10	73.7	78.0	73.2	74.8	0.0001 **	0.35
Postnatal day 2	71.1	72.5	72.5	71.8	0.11	0.71

Europe PMC Funders Author Manuscripts

TABLE 2

Similarities and Differences Between *Pax6*$^{+/-}$ and *PAX77*$^{+}$ Eyes[a]

	Pax6$^{-/-}$	PAX77^{+}
Microphthalmia	Yes	Yes
Reduction of cell layers in corneal epithelium	Yes	Yes
Reduced epithelial thickness	Yes	No
Microcornea	No	Yes
Absent or reduced irides	Yes	No
Irides cystic and thickened	No	Yes
Absence of ciliary bodies	No	Yes
Presence of goblet cells	Yes	No
Increased BrdU expression	Yes	Yes
Increased p63 expression	Yes	Yes
Decreased K12 expression	Yes	Yes
Corneal opacity	Yes	No
Slowed wounding response	Yes	Yes
Wound healing improved by EGF addition	Yes	No

[a]BrdU, bromodeoxyuridine; EGF, epidermal growth factor.